Nanba, O., & Satoh, K. (1987) *Proc. Natl. Acad. Sci. U.S.A. 84*, 109-112.
Nilsson, F., Andersson, B., & Jansson, C. (1990) *Plant Mol. Biol. 14*, 1051-1054.
Noren, G. H., Boerner, R. J., & Barry, B. (1991) *Biochemistry 30*, 3943-3950.
Oswald, A., Streubel, M., Ljungberg, U., Hermans, J., Eskins, K., & Westhoff, P. (1990) *Eur. J. Biochem. 190*, 185-194.
Pakrasi, H. B., Williams, J. G. K., & Arntzen, C. J. (1988) *EMBO J. 7*, 325-332.
Pakrasi, H. B., De Ciechi, P., & Whitmarsh, J. (1991) *EMBO J. 10*, 1619-1627.
Reddy, K. J., Webb, R., & Sherman, L. A. (1990) *Biotechniques 8*, 250-251.
Rippka, R., Deruelles, J., Waterbury, J. B., Herdman, M., & Stanier, R. Y. (1979) *J. Gen. Microbiol. 30*, 5387-5395.
Rögner, M., Chisholm, D. A., & Diner, B. A. (1991) *Biochemistry 30*, 5387-5395.
Saiki, R. K., Gelfand, D. H., Stoffel, S., Scharf, S. J., Higuchi, R. G., Horn, T. T., Mullis, K. B., & Erlich, H. A. (1985) *Science 230*, 1350-1354.
Satoh, K., Nakatani, H. Y., Steinback, K. E., Watson, J., & Arntzen, C. J. (1983) *Biochim. Biophys. Acta 724*, 142-150.
Studier, F. W., & Moffatt, B. A. (1986) *J. Mol. Biol. 189*, 113-130.
Szczepaniak, A., & Cramer, W. A. (1991) *EMBO J. 10*, 2757-2764.
Tabor, S., & Richardson, C. C. (1985) *Proc. Natl. Acad. Sci. U.S.A. 82*, 1074-1078.
Tabor, S., & Richardson, C. C. (1987) *Proc. Natl. Acad. Sci. U.S.A. 84*, 4767-4771.
Tae, G.-S. (1991) Ph.D. Thesis, Purdue University.
Tae, G.-S., & Cramer, W. A. (1989) *FEBS Lett. 259*, 161-164.
Tae, G.-S., Black, M. T., Cramer, W. A., Vallon, O., & Bogorad, L. (1988) *Biochemistry 27*, 9075-9080.
Vallon, O., Tae, G.-S., Cramer, W. A., Simpson, D., Hoyer-Hansen, G., & Bogorad, L. (1989) *Biochim. Biophys. Acta 975*, 132-141.
Vermaas, W. F. J., Ikeuchi, M., & Inoue, Y. (1988) *Photosynth. Res. 17*, 97-113.
Vermaas, W. F. J., Charite, J., & Shen, G. (1990) *Biochemistry 29*, 5325-5332.
Westhoff, P., Shrubar, H., Oswald, A., Streubel, M., & Offerman, K. (1990) *Current Research in Photosynthesis* (Baltscheffsky, M., Ed.) Vol. III, pp 483-490, Kluwer Academic Publishers, Dordrecht, The Netherlands.
Widger, W. R., Cramer, W. A., Hermodson, M., Meyer, D., & Gullifor, M. (1984) *J. Biol. Chem. 259*, 3870-3876.
Williams, J. G. K. (1988) *Methods Enzymol. 167*, 766-778.

Inactivation of Calcium Uptake by EGTA Is Due to an Irreversible Thermotropic Conformational Change in the Calcium Binding Domain of the Ca^{2+}-ATPase†

Kwan Hon Cheng* and James R. Lepock

Department of Physics, Texas Tech University, Lubbock, Texas 79409, and Departments of Physics and Biology, University of Waterloo, Ontario, Canada N2L 3G1

Received November 12, 1991; Revised Manuscript Received February 18, 1992

ABSTRACT: Calcium uptake by rabbit skeletal sarcoplasmic reticulum (SR) is inhibited with an effective inactivation temperature (T_I) of 37 °C in EGTA with no effect on ATPase activity. Since the Ca-ATPase denatures at a much higher temperature (49 °C) in EGTA, this suggests that a small or localized conformational change of the Ca-ATPase at 37 °C results in inability to accumulate calcium by the SR. Using a fluorescent analogue of dicyclohexylcarbodiimide, *N*-cyclohexyl-*N'*-[4-(dimethylamino)-α-naphthyl]-carbodiimide (NCD-4), the region of the calcium binding sites of the SR Ca-ATPase was labeled. Steady-state and frequency-resolved fluorescence measurements were subsequently performed on the NCD-4-labeled Ca-ATPase. Site-specific information pertaining to the hydrophobicity and segmental flexibility of the region of the calcium binding sites was derived from the steady-state fluorescence intensity, lifetime, and rotational rate of the covalently bound NCD-4 label as a function of temperature (0-50 °C). A reversible transition at ~15 °C and an irreversible transition at ~35 °C were deduced from the measured fluorescence parameters. The low-temperature transition agrees with the previously observed break in the Arrhenius plot of ATPase activity of the native Ca-ATPase at 15-20 °C. The high-temperature transition conforms well with the conformational transition, resulting in uncoupling of Ca translocation from ATP hydrolysis as predicted from the irreversible inactivation of Ca uptake at 31-37 °C in 1 mM EGTA. We conclude that an irreversible conformational change in the region of the calcium binding sites, of considerable lesser magnitude than unfolding, is responsible for the thermal inactivation of Ca uptake and uncoupling of Ca transport from ATP hydrolysis at elevated temperatures in EGTA.

The Ca transport function of the purified membrane-bound calcium adenosinetriphosphatase (Ca-ATPase) from muscle sarcoplasmic reticulum (SR) is quite sensitive to temperature with a significant inactivation of ATP-dependent Ca uptake of the Ca-ATPase at temperatures in excess of 30 °C when heated in the absence of calcium and in the presence of EGTA (McIntosh & Berman, 1978; Lepock et al., 1990). An inactivation temperature (T_I) of 37 °C is found for Ca uptake in 1 mM EGTA. Here T_I is defined as the temperature of

† This work was supported by USPHS Grants CA47610 to K.H.C. and CA40251 to J.R.L.

* Correspondence should be addressed to this author at the Biophysics Laboratory, Department of Physics, Box 4180, Texas Tech University, Lubbock, TX 79409-1051.

0006-2960/92/0431-4074$03.00/0

half-inactivation when the temperature is increased at 1 °C/min (Lepock et al., 1990). This inactivation is a form of uncoupling of calcium uptake from ATP hydrolysis since ATPase activity is not significantly inactivated until temperatures of 45–50 °C are reached (Cheng et al., 1987; Lepock et al., 1990). Membrane permeability is not increased in EGTA (Lepock et al., 1990); thus, inactivation of Ca uptake is not due simply to increased calcium leakiness. Other treatments that uncouple Ca uptake from ATP hydrolysis also do not increase the permeability of the SR membrane to calcium (Berman, 1982).

In EGTA, the Ca-ATPase denatures with a transition temperature of 49 °C, and the denaturation profile can be modeled very well assuming a two-state, irreversible, native to denatured transition (Lepock et al., 1990). Upon addition of calcium, the enzyme is stabilized, and two domains, one containing the nucleotide binding site and the other the transmembrane domain, can be detected. However, neither differential scanning calorimetry (DSC) nor fluorescence studies of fluorescein isothiocyanate (FITC)-labeled enzyme or intrinsic tryptophan fluorescence show a conformational or structural change between 30 and 40 °C that could be responsible for inactivation of Ca uptake (Lepock et al., 1990).

The kinetics of thermal inactivation of Ca uptake depend strongly on the concentrations of membrane cholesterol (Cheng et al., 1987), calcium (McIntosh & Berman, 1978; Cheng, 1989a; Lepock et al., 1990), and exogenously added cellular hyperthermic protectors (e.g., glycerol) and sensitizers (e.g., local anesthetics) (Cheng et al., 1987). In contrast, the inactivation of Ca-dependent ATP hydrolysis activity has an inactivation temperature T_I of approximately 49 °C and is 10-fold less sensitive to cholesterol, calcium, and other chemicals than inactivation of Ca uptake (Cheng et al., 1987; Lepock et al., 1990). The observed differential heat sensitivity of Ca uptake and ATP hydrolysis leads us to hypothesize that the impairment mechanisms governing the two activities are different from one another.

This differential impairment model is consistent with the proposed tertiary structure of the Ca-ATPase as predicted from the primary sequence (Clark et al., 1989; MacLennan, 1990). According to this structural model, the Ca translocation and ATP hydrolysis sites are located in different structural domains of the protein. Thus, denaturation or impairment of a specific structural domain within the protein must be related to and responsible for the functional inactivation associated with that domain. The calcium binding sites are in the Ca transport domain which is located in the transmembrane region of the protein. Two calcium ions bind to the high-affinity binding sites in this transport domain. When the energy derived from the hydrolysis of ATP is utilized, a conformational change of the protein results in exposure of the calcium binding sites to the lumen and an alteration of the affinity of bound calcium, resulting in the translocation of calcium from the cytoplasmic side to the lumen.

In order to test the above differential impairment model, various physical techniques, including differential scanning calorimetry (DSC) (Lepock et al., 1990) and fluorescence spectroscopy (Cheng, 1989a; Lepock et al., 1990), have been employed. Recent results from DSC measurements on the native Ca-ATPase and fluorescence intensity measurements on the FITC-labeled Ca-ATPase reveal that the unfolding of the ATP binding domain is responsible both for the thermal inactivation of ATP hydrolysis at around 49 °C and for inactivation of Ca uptake with the same inactivation temperature in 1 mM calcium (Lepock et al., 1990). Yet the impairment mechanism of Ca transport in EGTA which occurs at a much lower temperature (T_I = 37 °C in the absence of calcium) has not been identified.

In an attempt to detect the proposed heat-induced conformational alteration of the Ca transport domain, site-specific fluorescent labeling of the region of the calcium binding sites of the Ca-ATPase was performed using *N*-cyclohexyl-*N'*-[4-dimethylamino)-α-naphthyl]carbodiimide (NCD-4). NCD-4 is a fluorescent analogue of carbodiimide (DCCD). It has been established by Garcia de Anios and Inesi (1988) that DCCD labels both the proteolytic A_1 and A_2 fragments of the Ca-ATPase in the presence of calcium. Recently, Sumbilla et al. (1991) have found that NCD-4 specifically labels the A_1 fragment in the absence of calcium. Since the A_1 fragment is associated with the intramembranous portion of the Ca-ATPase (Clark et al., 1989), it was therefore suggested that NCD-4 labels the regions at or near the two calcium binding sites of the Ca-ATPase and possibly some nonspecific sites in the absence of calcium (Sumbilla et al., 1991). It has further been shown (Munkonge et al., 1989) that the NCD-4 labeling sites are close to each other as demonstrated by the identical resonance energy-transfer behavior between the NCD-4 labels and fluorescent-labeled lipids in the absence or presence of calcium. For convenience, the SR labeled in the absence of calcium is denoted as the specific labeled SR in this study while the SR labeled in the presence of calcium as the nonspecific labeled SR.

Fluorescence spectroscopy is a powerful technique to detect the structural conformation and rotational dynamics of the Ca-ATPase (Cheng, 1989a; Suzuki et al., 1989; Gryczynski et al., 1989). Steady-state and frequency-resolved fluorescence spectroscopic measurements of the NCD-4-labeled SR were carried out as a function of temperature in this study. From these fluorescence measurements, selective information pertaining to the alterations of the conformation, and specifically the hydrophobicity and rotational flexibility, of the region of the calcium binding sites within the Ca transport domain of the protein was obtained.

Materials and Methods

Ca-ATPase Isolation and Enzymatic Activities. Highly purified microsomal SR membranes were isolated in the presence of dithiothreitol from the hind leg and back muscles of New Zealand White rabbits as described previously (Cheng et al., 1986; Cheng & Hui, 1986; Campbell et al., 1980; MacLennan, 1970). The purified SR was found to contain more than 90% (w/w) of the Ca-ATPase (M_r = 110000) (Cheng et al., 1986; Cheng, 1989a). ATP-dependent Ca uptake of SR was measured by monitoring the absorbance of arsenazo III, a calcium-sensitive metallochromic dye, at 660 nm as described by Herbette et al. (1977). Calcium-dependent ATP hydrolysis activity of SR was determined using a coupled enzyme system as described by Warren et al. (1974).

Fluorescent Labeling of the Calcium Binding Sites of the Ca-ATPase. Fluorescent labeling of the calcium binding sites of the Ca-ATPase was performed according to methods described by Chadwick and Thomas (1983, 1984) with a few modifications. Briefly, SR membranes were incubated at 4 °C in a low-pH buffer [100 mM KCl/50 mM sodium 2-(*N*-morpholino)ethanesulfonic acid (NaMES), at pH 6.2] in the presence of 1 mM EGTA or 1 mM $CaCl_2$ at a concentration of 1 mg/mL protein. A small amount of methanol containing NCD-4 was then added to the membrane suspension. The final concentration of methanol in the solution was always less than 0.1%. The fluorophore/membrane mixture was then incubated at 4 °C for 10 h in the dark. The pH of the mixture

was adjusted to 7.0 by addition of a small amount of high-pH buffer [500 mM sodium 3-(*N*-morpholino)propanesulfonic acid (NaMOPS), pH 8.0]. The mixture was further diluted 10-fold in a neutral buffer [100 mM KCl, 10 mM *N*-[tris(hydroxymethyl)methyl]-2-aminoethanesulfonic acid (TES), and 1 mM $CaCl_2$ or 1 mM EGTA, pH 7.0] and subsequently centrifuged at 50000*g* for 30 min. To further remove the unreacted NCD-4, the membrane pellet was resuspended in the above neutral buffer and passed through a Sephadex LH20 column.

Fluorescence Measurements. All steady-state and frequency-resolved fluorescence measurements were made on an ISS-Greg 200 multifrequency cross-correlation fluorometer (ISS Inc., Urbana, IL). A cw He–Cd laser (Liconix 4242NB) with an output of 17 mW at 325 nm was used as an excitation source.

For the fluorescence spectral measurements, excitation and emission slit widths were set at 4 nm. Scattering contributions, which were determined from a membrane suspension prepared under identical procedures and conditions but in the absence of fluorophores, were subtracted from the fluorescence signals. The total fluorescence intensity of each sample was determined by integrating the fluorescence spectrum from 350 to 600 nm.

For the steady-state fluorescence anisotropy (r) measurements, both excitation and emission polarizers were employed. A low-wavelength cutoff filter (Model 3-73; Corning Glass Works, Corning, NY) was used to remove the excitation light from the fluorescence signal. Here r is defined as $(I_\parallel - I_\perp)/(I_\parallel - 2I_\perp)$, where $I_\parallel$ and $I_\perp$ represent the corrected fluorescence emission intensities that are parallel and perpendicular to the polarization direction of the excitation laser beam, respectively. The details of the steady-state anisotropy measurements have been described elsewhere (Cheng et al., 1986; Cheng, 1989b).

For the fluorescence lifetime measurements, the phase shift $(\delta_F - \delta_S)$ and the demodulation ratio (M_F/M_S) of the fluorescence emission signal as compared with a nonfluorescent glycogen solution were measured at frequencies ranging from 1 to 150 MHz. Here M_F and M_S represent the intensity modulation values of the fluorescent sample and that of the reference, and δ_F and δ_S represent the phase delay of the signal from the fluorescence sample and that from the reference sample. The same low-wavelength cutoff filter was used for the detection of fluorescence, and no filter was used for the reference sample. Since the light exiting from the pockels cell (electrooptical device) is vertically polarized, a polarizer with polarization axis set at 35° with respect to the vertical was placed in the excitation beam to eliminate the contribution of rotational diffusion of the sample to the measurements. The fluorescence lifetimes of the samples were deduced by fitting the frequency domain data with an exponential decay law using a nonlinear least-squares method (Lakowicz et al., 1984; Cheng, 1989b). The exponential decay law has a form of

$$I(t) = \sum \alpha_i \exp(-t/\tau_i) \quad (1)$$

where $I(t)$ is the fluorescence intensity decay and α_i is the molar fraction of the ith component with a fluorescence lifetime of τ_i. With this expression, the single- and double-exponential decays correspond to the maximum values of $i = 1$ and $i = 2$, respectively.

A rotational parameter, Y, was also employed to quantitate the rotational dynamics of NCD-4. It has been shown that Y is inversely related to the microviscosity of the environment as seen by the fluorophore (Weber et al., 1984) and can be expressed by the equation:

$$Y = \log [(r_0/r) - 1] - \log (RT\tau/v) \quad (2)$$

where r_0, R, T, τ, and V represent the initial anisotropy, universal gas constant, absolute temperature, average fluorescence lifetime, and effective volume of the fluorophore, respectively. As seen in eq 2, Y can be calculated if the values of τ and r are known. A detailed description of the physical meaning of Y can be found elsewhere (Weber et al., 1984).

Fitting Criterion and Errors. The best fitting of the frequency domain data to the model given above was based on the minimization of the reduced χ^2 parameter using a nonlinear least-squares procedure. The fitting errors were calculated by using the propagation of errors from the original frequency domain data to the derived parameters during the χ^2 minimization process (Gratton et al., 1984).

Thermal Inactivation. The SR at 600–700 μg of protein/mL was heated in a solution of 100 mM KCl, 5 mM dithiothreitol, pH 7.0, and 1 mM EGTA. The SR at twice the concentration desired was added to a preheated test tube at the inactivation temperature (34–38 °C) containing an equal volume of the same solution. In this way, thermal equilibrium was achieved in 1–2 min. Samples were removed at regular intervals and immediately added to the Ca uptake solution. Ca uptake activity was directly proportional to the amount of SR added over the range of activities measured. The rate of inactivation was obtained from a least-squares analysis of the plot of ln activity vs time at the elevated temperature. The activation energy (E_A) and constant (A) of the Arrhenius relation were obtained from the slope and intercept of an Arrhenius plot which was linear from 34 to 38 °C (Lepock et al., 1990).

The fractional inactivation (f_D) of calcium uptake as a function of temperature increasing at a rate of 0.2 °C/min was calculated and compared to the fractional change in the fluorescence parameters measured under the same conditions. The linear Arrhenius plot implies that

$$k(T) = e^{A - E_A/RT} \quad (3)$$

where k is the rate of denaturation, E_A the activation energy, and A a constant containing the entropy of inactivation. Irreversible denaturation, following pseudo-first-order kinetics, at a constant temperature as a function of time is described by the differential equation:

$$df_D(t)/dt = k(T)[1 - f_D(t)] \quad (4)$$

where f_D is the fraction denatured, T the temperature, and t the time. If the temperature is no longer constant, then the function $f_D[T(t)]$ as a function of time while temperature is scanned at a constant rate is found by replacing k in eq 4 with the Arrhenius relation (eq 3) and letting $T = T_0 + vt$ where v is the scan rate and T_0 the starting temperature. The resulting equation:

$$df_D[T(t)]/dt = e^{A - E_A/R(T_0+vt)}(1 - f_D[T(t)]) \quad (5)$$

can be solved and an approximate solution (eq 6) obtained (Lepock et al., 1990) where T_c is the temperature at which $k = 1$. Equation 6 was used to calculate the fractional inactivation of calcium uptake shown in Figure 7. The transition or inactivation temperature is defined as the temperature at which $f_D = 0.5$.

$$f_D[T(t)] = 1 - \exp\left\{\frac{-RT_c^2}{E_A v} \exp\left[\frac{E_A}{RT_c^2}(T - T_c)\right]\right\} \quad (6)$$

Results

Fluorescent Labeling of the SR Ca-ATPase. The SR Ca-ATPase was labeled with NCD-4 both in the absence and in

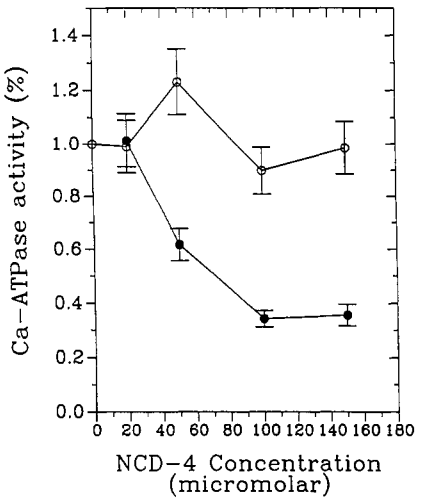

FIGURE 1: Normalized calcium-dependent ATP hydrolysis activity of the NCD-4-labeled SR as a function of the concentration of free NCD-4 during labeling. The activities of the Ca-ATPase labeled in the presence (○) and absence (●) of 1 mM $CaCl_2$ are shown. All activity measurements were performed at 23 °C. Each point represents an average of the results from four independent labeling experiments with the bar indicating the standard error.

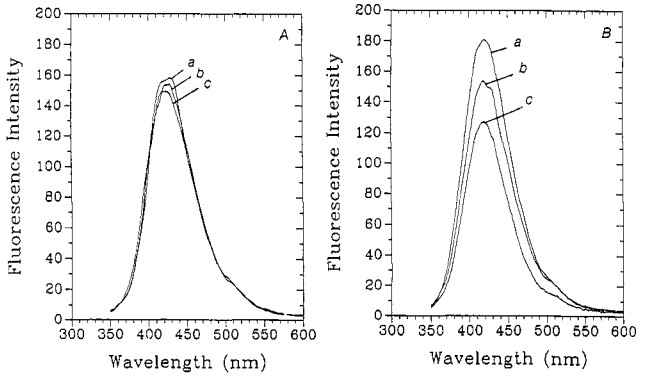

FIGURE 2: Uncorrected steady-state fluorescence spectra of the nonspecific NCD-4-labeled SR (panel A) and specific labeled SR (panel B) in the presence of (a) 0, (b) 0.3, and (C) 1 mM $CaCl_2$ at 4 °C. The excitation wavelength was at 325 nm, and the emission wavelength was varied from 350 to 600 nm with a resolution of 4 nm.

the presence of calcium (1 mM $CaCl_2$). Figure 1 shows the calcium-dependent ATP hydrolysis activity of the labeled Ca-ATPase as a function of the free concentration of NCD-4 added to the SR during the labeling. For the SR labeled in the absence of calcium (1 mM EGTA), the calcium-dependent ATP hydrolysis activity was found to decline progressively as the concentration of NCD-4 increased. However, for the SR labeled in the presence of calcium, the activity was not inhibited up to 160 μM NCD-4. As mentioned in the introduction, the SR labeled in the absence of calcium is denoted as the specific labeled SR and that in the presence of calcium as the nonspecific labeled SR.

Calcium Response of the Fluorescence Parameters of the NCD-4-Labeled SR. The response of various steady-state and frequency-resolved fluorescence parameters of the specific and nonspecific NCD-4-labeled SR was determined in order to establish the site specificity of NCD-4 labeling. In these fluorescence studies, the free concentration of NCD-4 used during the labeling was fixed at 70 μM, and all fluorescence measurements were performed at 4 °C.

Figure 2 shows the fluorescence spectra of the NCD-4-labeled SR in buffers containing various concentrations of calcium (0, 0.3, and 1 mM). The fluorescence spectrum of the nonspecific labeled SR has a maximum at around 430 nm.

Table I: Fluorescence Parameters of the NCD-4 (both Specific and Nonspecific)-Labeled SR in the Presence or Absence of Calcium at 4 °C

sample	τ_L[a] (10^{-9} s)	τ_S[b] (10^{-9} s)	α_L[c]
specific labeled SR			
0 mM $CaCl_2$	6.91 ± 0.42	1.41 ± 0.10	0.24 ± 0.04
1 mM $CaCl_2$	5.32 ± 0.35	0.69 ± 0.20	0.29 ± 0.04
nonspecific labeled SR			
0 mM $CaCl_2$	5.89 ± 0.27	1.99 ● 0.27	0.56 ± 0.03
1 mM $CaCl_2$	5.28 ± 0.17	1.59 ± 0.26	0.62 ± 0.04

[a] Resolved long fluorescence lifetime component of the NCD-4-labeled SR. [b] Resolved short fluorescence lifetime component of the NCD-4-labeled SR. [c] Molar fraction of the long fluorescence lifetime component of the NCD-4-labeled SR.

This fluorescence peak decreased slightly (<5%) as the calcium concentration increased (Figure 2A). On the other hand, the intensity of the fluorescence spectrum of the specific labeled SR showed a strong dependence on the concentration of calcium. As shown in Figure 2B, the peak of the fluorescence spectrum decreased by more than 20 and 30% in the presence of 0.3 and 1 mM $CaCl_2$, respectively.

Fluorescence lifetime measurements on the NCD-4-labeled SR were performed, and the results are presented in Table I. Both single-exponential and double-exponential decay functions (see eq 1) were used to fit the frequency domain data. Only the double-exponential decay function was able to fit the data successfully, as judged by the observation that the χ^2 of the double-exponential fit was almost 2-fold less than that of the single-exponential fit. Also, both triple-exponential and continuous distribution fits were employed to fit the data with very little improvement in the χ^2 values. Thus, a double-exponential function is adequate. For the specific labeled SR, the two resolved fluorescence lifetimes were approximately 6.9 and 1.4 ns. For the nonspecific labeled SR, the lifetimes were 5.9 and 2.0 ns. In the presence of 1 mM $CaCl_2$, the fluorescence lifetimes of the specific labeled SR dropped significantly to 5.3 and 0.69, while a smuch smaller change in the lifetimes of the nonspecific labeled SR was detected. For all labeled SR, the molar fractions of the two lifetime components were found to be insensitive to the addition of calcium. These results support the previous studies (Chadwich & Thomas, 1983, 1984; Munkonge et al., 1989) showing that NCD-4 labels are close to the calcium binding sites or in a region of the protein whose conformation is highly sensitive to calcium binding.

Thermal Response of the Fluorescence Parameters of NCD-4-Labeled SR. The thermal response of the region of the Ca-ATPase containing the calcium binding sites of the specific labeled SR was evaluated by measuring the steady-state and frequency-resolved fluorescence parameters of the covalently bound NCD-4 as a function of temperature from 0 to 50 °C at a heating rate of approximately 0.2 °C/min. The heating rate is important for quantitative evaluation of irreversible transitions since the extent of the transition is dependent on both temperature and time of exposure (Lepock et al., 1990).

Figure 3 shows the steady-state fluorescence intensity of the NCD-4 specific labeled SR as a function of temperature. In the absence of calcium, a gradual decline (~30%) in the fluorescence intensity was found as the temperature increased from 0 to 20 °C. Thereafter, the intensity remained essentially constant as the temperature changed from 20 to 35 °C. An abrupt transition was then observed starting at 32 °C and ending at 43 °C. The fluorescence intensity decreased by more than 70% during this transition. In the presence of calcium, a similar temperature dependence of the fluorescence intensity

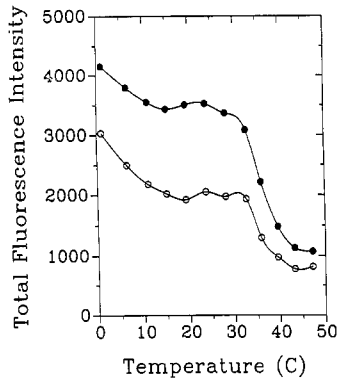

FIGURE 3: Steady-state total fluorescence intensity of the NCD-4 specific labeled SR as a function of temperature in the presence (○) and absence (●) of 1 mM $CaCl_2$. The value of fluorescence intensity was calculated by integrating the fluorescence emission spectrum of labeled SR from 350 to 600 nm.

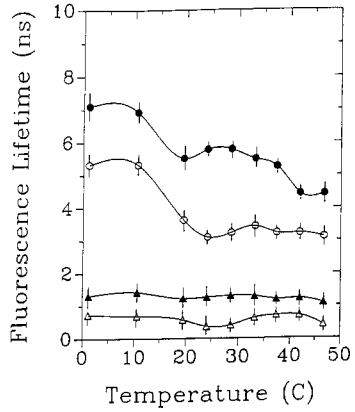

FIGURE 4: Resolved fluorescence lifetimes, long (circles) and short (triangles) lifetime components, of the NCD-4 specific labeled SR as a function of temperature in the presence (open symbols) and absence (filled symbols) of 1 mM $CaCl_2$. The bars indicate fitting errors from the nonlinear least-squares fit of the frequency domain data.

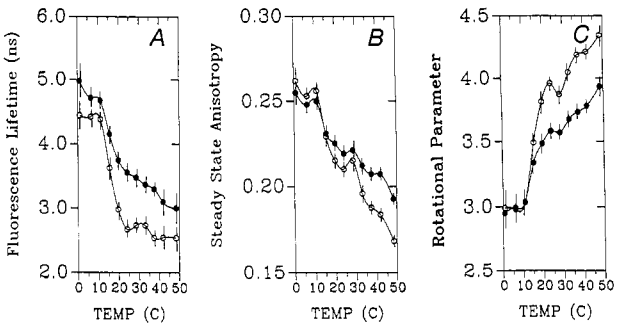

FIGURE 5: Average fluorescence lifetime (panel A), steady-state anisotropy (panel B), and rotational parameter Y (panel C) of the NCD-4 specific labeled SR as a function of temperature in the presence (open symbols) and absence (filled symbols) of 1 mM $CaCl_2$. The uncertainties of the parameters are indicated by the bars in the graphs.

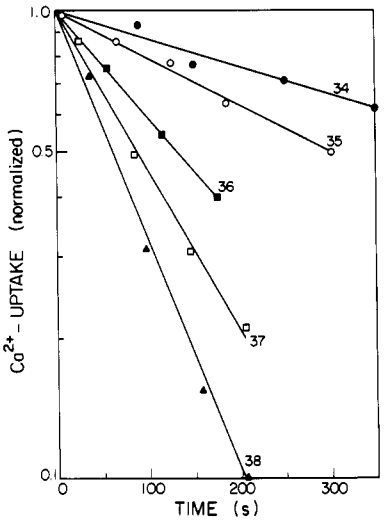

FIGURE 6: Inactivation of Ca uptake of SR heated in EGTA at 34–38 °C. Normalized Ca uptake as a function of time of exposure at constant temperature is plotted.

was also found. Note that the intensity of the NCD-4-labeled SR in the presence of calcium was always lower than that in the absence of calcium.

Fluorescence lifetimes of NCD-4 in the specific labeled SR as a function of temperature were also measured and are shown in Figure 4. The long fluorescence lifetime component exhibited strong temperature dependence while the short component was relatively insensitive to temperature. For the long component, two transitions centered at around 15 and 35 °C were observed in the absence of calcium. In the presence of calcium, the transition at 15 °C was evident, but no significant change occurred at higher temperatures. The relative fraction of the long-lifetime component was approximately 0.3 and independent of temperature.

The segmental flexibility of the covalently bound NCD-4 was also studied as a function of temperature. A rotational parameter, Y, was employed to quantitate the rotational behavior of NCD-4. This rotational parameter was calculated from the average fluorescence lifetime and steady-state anisotropy of NCD-4 using eq 2 as described under Materials and Methods. The average lifetime, τ_{avg}, was calculated from the resolved lifetime components and their relative molar fractions using the formula $\tau_{avg} = \sum f_i \tau_i$ where $f_i = \alpha_i \tau_i / \sum \alpha_i \tau_i$ (Lakowicz et al., 1984). As shown in Figure 5A,B, both the average fluorescence lifetime and the steady-state anisotropy of NCD-4 exhibited a sharp transition centered at ~15 °C and a very weak transition at ~35 °C. The transition at 15 °C was clearly present in the plot of the calculated rotational parameter Y, but the transition at 35 °C was poorly defined. As seen in Figure 5C, the rotational rate of NCD-4 in the presence of calcium was higher than that in the absence of calcium for temperatures higher than 20 °C. This suggests that the mobility of the NCD-4 binding domain increases upon binding to calcium. A similar calcium response was also found for the *N*-(1-anilinonaphth-4-yl)maleimide binding domain (Suzuki et al., 1989).

For all steady-state and frequency-resolved fluorescence measurements, the low-temperature transition at 15 °C was reversible. However, the high-temperature transition at ~35 °C was found to be irreversible; i.e., the transition at 35 °C was not present after the first heating to 50 °C followed immediately by rapid cooling.

Thermal Inactivation of Calcium Uptake. The thermal inactivation of calcium uptake in the presence of 1 mM EGTA was determined by measuring the activity at 25 °C after exposure to inactivating temperatures. Plots of fractional Ca uptake activity remaining as a function of time of exposure are given in Figure 6. Inactivation obeys pseudo-first-order kinetics, and the inactivation rates (k) were determined by linear regression analysis. A linear Arrhenius plot of the rate constant for inactivation of Ca uptake was obtained (results not shown). The values of E_A and A, obtained by linear regression analysis, were used to calculate f_D shown in Figure 7 using eq 6. The activation energy for thermal inactivation of Ca uptake is very high (400 kJ/mol), well into the range of activation energies normally observed for protein denatu-

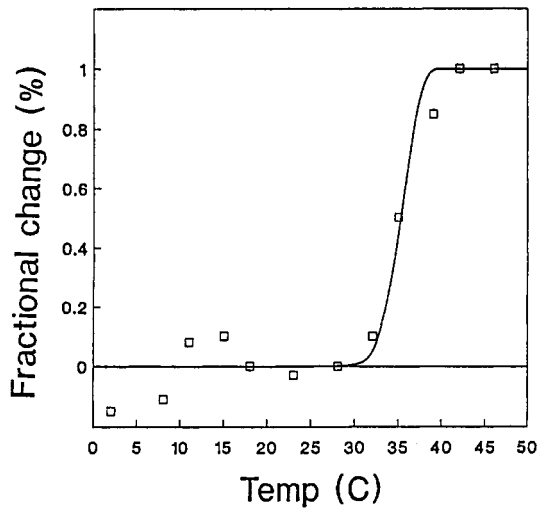

FIGURE 7: Predicted fractional inactivation of Ca uptake of the Ca-ATPase as a function of temperature at a temperature increase of 0.2 °C/min (solid line) and fractional change in the fluorescence intensity of the NCD-4 specific labeled SR (points) in EGTA. Calculations were performed as described in Lepock et al. (1990).

ration and other macromolecular transitions.

To confirm the positive correlation between inactivation of Ca uptake and the conformational change in the region of the calcium binding sites, the inactivation profile of Ca uptake of the native SR and the fractional change in fluorescence intensity of NCD-4 in the labeled SR were directly compared and are shown in Figure 7. The inactivation profile is the fraction of inactivated protein (f_D) versus temperature when the sample is heated at a specific rate, in this case 0.2 °C/min. The inactivation profile has a transition centered at around 35 °C, 2 °C lower than T_I for a heating rate of 1 °C/min. The fractional change in the fluorescence intensity, δF, of NCD-4 as a function of temperature was calculated and normalized as described in Lepock et al. (1990). As seen in Figure 7, the inactivation curve agrees well with the δF vs temperature data. Good fits were also obtained for the normalized change in fluorescence lifetime (results not shown). This analysis is based on the assumption that the fractional change in each parameter is equal to the fractional completion of the transition.

Discussion

The mechanism of impairment of Ca uptake of the Ca-ATPase at elevated temperatures has been investigated by the use of steady-state and frequency-resolved fluorescence spectroscopy. The hypothesis of this study is that slight irreversible alterations in the local conformation of the calcium binding site region or domain at elevated temperatures are sufficient to produce an inactivation of Ca uptake by the protein. According to the predicted tertiary structure model of the Ca-ATPase (Clark et al., 1989; MacLennan, 1990), the energy-dependent calcium transport process involves concerted movements of two or more α-helices of the Ca transport domain (MacLennan, 1990). Therefore, the conformation of the region containing the calcium binding sites within the Ca transport domain should play a crucial role in regulating the function of the enzyme.

In this study, the region of the calcium binding sites of the Ca-ATPase was labeled by NCD-4. The specificity of the labeling is supported by the sensitivity to calcium of several parameters of the NCD-4 specific labeled enzyme. The presence of calcium during labeling prevents the NCD-4-induced decline in calcium-dependent ATP hydrolysis which was observed during labeling of the SR in the absence of calcium. The sensitivity of the measured fluorescence parameters (steady-state intensity, lifetimes, and rotational rate) of the specific labeled SR to calcium confirms that the covalently attached NCD-4 fluorophores are probing a region highly sensitive to calcium binding to the Ca-ATPase. The calcium binding sites are thought to consist of Asp and Glu residues (Clark et al., 1989), and these residues are labeled by DCCD as well as NCD-4 (Garcia de Anios & Inesi, 1988; Munkonge et al., 1989).

It has been suggested that other nonspecific sites of the Ca-ATPase are also labeled by NCD-4 for the specific labeled SR (Chadwick & Thomas, 1984; Munkonge et al., 1989). The relative contributions of the fluorescence signal from these nonspecific sites as compared with those from the region of the calcium binding sites cannot be determined at this time. However, the locations of the nonspecific sites were shown to be very close to the specific sites (Munkonge et al., 1989), and the magnitude of the calcium-induced changes in the fluorescence parameters implies that a large fraction of the fluorescence is sensitive to calcium binding.

The microenvironment of the NCD-4 label in the Ca-ATPase is quite heterogeneous as evidenced by the existence of two distinctively different lifetimes of the covalently bound NCD-4. The two different lifetimes may reflect two major labeling sites within the Ca-ATPase. This dual-labeling hypothesis is also supported by the known stoichiometry of the NCD-4-labeled SR (bound probe/Ca-ATPase = 2:1) (Chadwick & Thomas, 1984); however, the possibility of more than two labeling sites within the Ca-ATPase cannot be eliminated with certainty based simply on the number of resolved lifetime components. The fluorescence lifetime measurements are only able to resolve two components. A triple-exponential fit and even continuous lifetime distribution function involving either one or two components did not improve the χ^2 values over the simple biexponential fit. However, more than one binding site may have similar lifetime characteristics, but the binding sites can still be classified into two categories on the basis of their lifetime characteristics.

The fluorescence lifetime of NCD-4 in the Ca-ATPase is a good indicator of the hydrophobicity of the environment where the probe is bound. The quantum yield of NCD-4 is solvent-sensitive (Chadwick & Thomas, 1983). Free NCD-4 is nonfluorescent unless it is attached to an acidic residue via its *N*-acetylurea group. This resulting product is analogous to 2-anilinonaphthalene, a precursor of the hydration-sensitive probe 1-anilinonaphthalene-8-sulfonate (8,1-ANS) (Cheng, 1990). From the hydration sensitivity and the likely existence of two binding sites, we conclude that the two NCD-4 labeling sites report two different local water structures at the binding sites and that one site is more hydrophobic than the other. The label of longer lifetime in the hydrophobic environment is sensitive to both transitions at 15 and 35 °C, while the less hydrophobic label is sensitive to neither. This observation leads us to suggest that the hydrophobic label is able to reflect subtle alterations in the conformation of the region containing the calcium binding sites. This label is less accessible to solvent and may be located in the transmembrane region or between the stalks of helices above the lipid bilayer surface. Both of these regions contain potential labeling sites consisting of Asp and Glu residues (Clark et al., 1989).

The steady-state fluorescence intensity of NCD-4 in the specific labeled SR exhibits transitions at 15 and 35 °C. Although the intensity can be measured with sufficient accuracy, the fluorescence intensity alone cannot reveal the

heterogeneous environment of the labels in the Ca-ATPase.

The segmental flexibility of the region of the calcium binding sites is reflected by the measured rotational parameter Y of NCD-4. The large increase in the value of the rotational parameter at 10–20 °C signifies a major increase in the rotational flexibility of NCD-4 in the region of the calcium binding sites at those temperatures. This change is centered at 15 °C. Interestingly, no significant change in the rotational motion of NCD-4 in the region of 35 °C is evident, indicating that the motional flexibility of the labeled region of the calcium binding sites is not significantly altered at that temperature.

Both major transitions at ~15 and 35 °C, inferred from the fluorescence measurements on NCD-4 in the specific labeled SR, correspond to changes in enzyme activity. The low-temperature reversible transition correlates well with the break in the Arrhenius plot of ATPase activity in the native Ca-ATPase at 15–20 °C (Bigelow et al., 1989). Our fluorescence results therefore suggest that a conformational change in the region of the calcium binding sites of the Ca-ATPase at ~15 °C is responsible for the observed change in the enzymatic activity of the protein at that temperature. Both the hydrophobicity and rotational flexibility of the region of the calcium binding sites are altered during the transition. A previous vibrational spectroscopic study (Mendelsohn et al., 1984) on the native Ca-ATPase reported that the ATPase transition at 15–20 °C is related to a conformational change of the protein and not with the lipid matrix. The irreversible transition at 35 °C corresponds to another conformational change of the Ca-ATPase in the region of the calcium binding sites. Only the hydrophobicity, not the rotational flexibility, of the region of the calcium binding sites is changed during this high-temperature irreversible transition.

The match between the inactivation of Ca uptake and the fluorescence parameters of NCD-4 suggests that local alterations in the region of the Ca-ATPase containing the calcium binding sites are responsible for the irreversible inactivation of Ca uptake at elevated temperatures. Specifically, the region of the calcium binding sites becomes more hydrophilic due to the transition at ~35 °C. Note that the ATP hydrolysis activity remains fully active until the temperature approaches 50 °C (Cheng, 1989a; Lepock et al., 1990). Therefore, the inactivation of Ca uptake signifies the uncoupling of Ca transport from ATP hydrolysis starting at ~30 °C. Our results therefore support the differential impairment model of inactivation of the Ca-ATPase and further indicate that the Ca transport domain is more heat-labile that the ATP hydrolytic domain.

In summary, this study demonstrates that the conformation of the region containing the calcium binding sites undergoes two structural transitions at 15 and 35 °C in addition to a much greater conformational change during denaturation or unfolding at 50 °C. The low-temperature transition is reversible and correlates with the break in the temperature-dependent behavior of ATPase activity at 15–20 °C. The high-temperature transition is irreversible and appears to be responsible for the thermal-induced impairment of Ca uptake and uncoupling of Ca transport from ATP hydrolysis of the Ca-ATPase at elevated temperatures in the absence of calcium (presence of EGTA).

References

Berman, M. C. (1982) *Biochim. Biophys. Acta 694*, 95–121.

Bigelow, D. J., Squier, T. C., & Thomas, D. D. (1986) *Biochemistry 25*, 194–202.

Campbell, K. P., Franzini-Armstrong, C., & Shamoo, A. E. (1980) *Biochim. Biophys. Acta 602*, 97–105.

Chadwick, C. C., & Thomas, E. W. (1983) *Biochim. Biophys. Acta 730*, 201–206.

Chadwick, C. C., & Thomas, E. W. (1984) *Biochim. Biophys. Acta 769*, 291–296.

Cheng, K. H. (1989a) *Cancer Res. 49*, 7026–7033.

Cheng, K. H. (1989b) *Biophys. J. 56*, 1251–1257.

Cheng, K. H. (1990) *Chem. Phys. Lipids 55*, 191–202.

Cheng, K. H., & Hui, S. W. (1986) *Arch. Biochem. Biophys. 244*, 382–386.

Cheng, K. H., Lepock, J. R., Hui, S. W., & Yeagle, P. L. (1986) *J. Biol. Chem. 261*, 5081–5087.

Cheng, K. H., Hui, S. W., & Lepock, J. R. (1987) *Cancer Res. 47*, 1255–1262.

Clark, D. M., Loo, T. W., Inesi, G., & MacLennan, D. H. (1989) *Nature 339*, 476–478.

Garcia de Anios, J., & Inesi, G. (1988) *Biochemistry 27*, 1793–1803.

Gratton, E., Jameson, D. M., & Hall, R. D. (1988) *Annu. Rev. Biophys. Bioeng. 13*, 105–124.

Gryczynski, I., Wiczk, W., Inesi, G., Squier, T., & Lakowicz, J. R. (1989) *Biochemistry 28*, 3490–3498.

Herbette, L., Marquardt, J., Scarpa, A., & Blasie, J. K. (1977) *Biophys. J. 20*, 245–272.

Lakowicz, J. R., Laczko, G., Cherek, H., Gratton, E., & Limkeman, M. (1984) *Biophys. J. 46*, 463–478.

Lepock, J. R., Rodahl, M., Zhang, C., Heynen, M. L., Waters, B., & Cheng, K. H. (1990) *Biochemistry 29*, 681–689.

MacLennan, D. H. (1970) *J. Biol. Chem. 245*, 4508–4518.

MacLennan, D. H. (1990) *Biophys. J. 58*, 1355–1366.

McIntosh, D. B., & Berman, M. C. (1978) *J. Biol. Chem. 253*, 5140–5146.

Mendelsohn, R., Anderle, G., Jaworsky, M., Mantsh, H. H., & Dluhy, R. A. (1984) *Biochim. Biophys. Acta 775*, 215–224.

Munkonge, F., East, J. M., & Lee, A. G. (1989) *Biochim. Biophys. Acta 979*, 113,120.

Sumbilla, C., Cantilina, T., Collins, J. H., Malak, H., Lakowicz, J. R., & Inesi, G. (1991) *J. Biol. Chem. 266*, 12682–12689.

Suzuki, S.-I., Kawato, S., Kouyama, T., Kinosita, K., Ikegami, A., & Kawakita, M. (1989) *Biochemistry 28*, 7734–7740.

Warren, G. B., Toon, P. A., Birdsall, J. M., Lee, A. G., & Metcalfe, J. C. (1974) *Proc. Natl. Acad. Sci. U.S.A. 71*, 622–626.

Weber, G., Scarlata, S., & Rholam, M. (1984) *Biochemistry 23*, 6785–6788.